Phys. Lett. B 849 (2024) 138452

Contents lists available at ScienceDirect

Physics Letters B

journal homepage: www.elsevier.com/locate/physletb

Letter

Magnetic moments of thallium isotopes in the vicinity of magic $N = 126$

Z. Yue [a,*], A.N. Andreyev [a,b], A.E. Barzakh [c], I.N. Borzov [c], J.G. Cubiss [a], A. Algora [d], M. Au [b,e], M. Balogh [f], S. Bara [g], R.A. Bark [h], C. Bernerd [b,g], M.J.G. Borge [i], D. Brugnara [f], K. Chrysalidis [b], T.E. Cocolios [g], H. De Witte [g], Z. Favier [b], L.M. Fraile [j], H.O.U. Fynbo [k], A. Gottardo [f], R. Grzywacz [l], R. Heinke [b], A. Illana [j,m,n], P.M. Jones [h], D.S. Judson [o], A. Korgul [p], U. Köster [b,q], M. Labiche [r], L. Le [b], R. Lica [b,s], M. Madurga [l], N. Marginean [s], B. Marsh [b], C. Mihai [s], E. Nácher [d], C. Neacsu [s], C. Nita [s], B. Olaizola [b,i], J.N. Orce [t], C.A.A. Page [a], R.D. Page [o], J. Pakarinen [b,m,n], P. Papadakis [r], G. Penyazkov [c], A. Perea [i], M. Piersa-Siłkowska [b,p], Zs. Podolyák [b,u], S.D. Prosnyak [c], E. Reis [b,v], S. Rothe [b], M. Sedlak [f], L.V. Skripnikov [c], C. Sotty [s], S. Stegemann [b], O. Tengblad [i], S.V. Tolokonnikov [c], J.M. Udías [j], P. Van Duppen [g], N. Warr [w], W. Wojtaczka [g]

[a] School of Physics, Engineering and Technology, University of York, York, YO10 5DD, United Kingdom
[b] CERN, 1211 Geneva 23, Switzerland
[c] Affiliated with an institute covered by a cooperation agreement with CERN
[d] Instituto de Fisica Corpuscular, CSIC-Universidad de Valencia, E-46071 Valencia, Spain
[e] Johannes Gutenberg-Universität, Saarstr. 21, 55099 Mainz, Germany
[f] INFN, Laboratori Nazionali di Legnaro (LNL), Viale dell'Università 2, 35020 Legnaro (PD), Italy
[g] Instituut voor Kern- en Stralingsfysica, KU Leuven, B-3001, Leuven, Belgium
[h] iThemba LABS, National Research Foundation, P.O. Box 722, Somerset West 7129, South Africa
[i] Instituto de Estructura de la Materia, CSIC, 28006 Madrid, Spain
[j] Grupo de Física Nuclear and IPARCOS, Universidad Complutense de Madrid, CEI Moncloa, E-28040 Madrid, Spain
[k] Department of Physics and Astronomy, Aarhus University, DK-8000 Aarhus C, Denmark
[l] Department of Physics and Astronomy, University of Tennessee, Knoxville, TN 37966, USA
[m] Department of Physics, University of Jyväskylä, P.O. Box 35, FI-40014, Jyväskylä, Finland
[n] Helsinki Institute of Physics, University of Helsinki, P.O. Box 64, FIN-00014, Helsinki, Finland
[o] Oliver Lodge Laboratory, University of Liverpool, Liverpool, L69 7ZE, United Kingdom
[p] Faculty of Physics, University of Warsaw, Warsaw, PL 02-093, Poland
[q] Institut Laue-Langevin, F-38042, Grenoble, France
[r] STFC Daresbury Laboratory, Daresbury, WA4 4AD, Warrington, United Kingdom
[s] Horia Hulubei National Institute of Physics and Nuclear Engineering (IFIN-HH), R-077125, Bucharest, Romania
[t] Department of Physics, University of the Western Cape, P/B X17 Bellville 7535, South Africa
[u] Department of Physics, University of Surrey, Guildford, GU2 7XH, United Kingdom
[v] Universität Duisburg–Essen, Duisburg, Germany
[w] Institut für Kernphysik, Universität zu Köln, Köln, D-50937, Germany

ARTICLE INFO

Editor: B. Blank

Keywords:
Laser spectroscopy
Hyperfine structure
Magnetic dipole moments
Theory of finite Fermi systems

ABSTRACT

The magnetic dipole moments (μ) of ^{209}Tl^{g} ($N = 128$) and ^{207}Tl^{m} ($N = 126$) have been measured for the first time using the in-source laser resonance-ionization spectroscopy technique with the Laser Ion Source and Trap (LIST) at ISOLDE (CERN). The application of the LIST suppresses the usually overwhelming background of the isobaric francium isotopes and allows access to heavy thallium isotopes with $A \geqslant 207$. The self-consistent theory of finite Fermi systems based on the energy density functional by Fayans et al. well describes the N dependence of μ for $1/2^+$ thallium ground states, as well as μ for the $11/2^-$ isomeric states in europium, gold and thallium isotopes.

* Corresponding author.
E-mail address: zixuan.yue@cern.ch (Z. Yue).

https://doi.org/10.1016/j.physletb.2024.138452
Received 20 July 2023; Received in revised form 15 November 2023; Accepted 8 January 2024
Available online 17 January 2024

The inclusion of particle-vibration coupling leads to a better agreement between the theory and experiment for $\mu(\mathrm{Tl}^g, I^\pi = 1/2^+)$. It is shown that beyond mean-field contributions to μ cannot be neglected at least for thallium isotopes with $I^\pi = 1/2^+$.

1. Introduction

Nuclear magnetic dipole moments (μ) provide direct information on the single-particle degrees of freedom in the nucleus and the underlying configurations of the valence nucleons [1]. Due to this, they are widely used to test the validity of nuclear theories (see, e.g. [2,3]). Of particular importance are data on the magnetic moments of states in doubly magic ±1 particle nuclei. The μ value in these cases is expected to be determined by the last occupied single particle orbit (Schmidt moment, see Refs. [4–6] and references therein). However, in the majority of cases, the observed μ values strongly deviate from the Schmidt predictions. This deviation can serve as a sensitive probe for the polarization induced by the unpaired valence nucleons, meson-exchange currents in nuclear medium and multiparticle excitations (see, for example, Ref. [5] and references therein). The doubly magic ±1 particle nuclei have simpler structure in comparison with other isotopes with odd number of protons or neutrons, therefore, the failure of the theory in their description can be more confidently connected with definite drawbacks in accounting for one or the other mechanism of the departure from the Schmidt value.

There were many attempts to describe theoretically μ for near-magic nuclei (see examples below in this Section). Nevertheless, some problems still remain, and new experimental data as well as theoretical analysis are necessary to obtain a self-consistent and comprehensive picture. In the present work we take a step toward this goal by studying nuclei in close vicinity to doubly-magic ^{208}Pb.

The magnetic moment of the $I^\pi = 1/2^+$ ground state of ^{207}Tl ($N = 126$, $Z = 81$) was first measured nearly four decades ago (1.869(5) μ_N [7,8]) with a strong deviation from the Schmidt value (2.793 μ_N) and since then it was extensively used to test various approaches to μ calculation (see e.g. the recent studies [9,10]). However, there is a long-lived ($T_{1/2} = 1.33$ s) $I^\pi = 11/2^-$ isomer $^{207}\mathrm{Tl}^m$ with an unknown μ value, which is expected to be well described by a single-hole configuration based on the $\pi h_{11/2}$ orbital. In contrast with the $\pi s_{1/2}$ ground state, which could have an appreciable contribution from other configurations, the $\pi h_{11/2}$ orbit is a unique-parity state, thus is expected to have less mixing with other configurations. Therefore, different theoretical mechanisms can be tested by comparison with experiment for these two nuclear states.

The measurement of $\mu(^{207}\mathrm{Tl}^g)$ also revealed a marked discontinuity in the μ isotopic trend for thallium ground states with $I^\pi = 1/2^+$. A noticeable drop was found when going from $^{207}\mathrm{Tl}^g$ to $^{205}\mathrm{Tl}^g$ (from 1.88 μ_N to 1.64 μ_N) [7,11], whereas for odd-A $^{179-205}\mathrm{Tl}^g$ isotopes, μ remains nearly constant (between 1.60 μ_N and 1.64 μ_N; [12–14]). A similar reduction relative to $^{207}\mathrm{Tl}^g$ is expected for $^{209}\mathrm{Tl}^g$ ($N = 128$) due to presumably the same underlying effect of the particle-vibration coupling [11].

This letter reports on the first measurement of μ for $^{207}\mathrm{Tl}^m$ and $^{209}\mathrm{Tl}^g$ with laser resonance-ionization spectroscopy at ISOLDE (CERN) [15] using the laser ion source and trap (LIST) [16–18]. The latter allowed production of isobarically-clean beams of thallium which was the key for the success of these measurements.

Several self-consistent μ calculations based on different energy-density functionals (EDF) were performed previously, such as the relativistic point-coupling model (see Refs. [6,19] and references therein), and Skyrme-Hartree-Fock Random Phase Approximation (RPA) calculations (see Ref. [20] and references therein). These and similar approaches restrict themselves as a rule to near-magic nuclei, and their applicability to the description of μ in long isotopic chains is not obvious.

Recent deformed EDF (DEDF) calculations with symmetry-restored wave functions and accounting for the time-odd terms in the functional, tackle the μ-problem in an alternative way without going beyond the mean field level [9]. In Refs. [21–23], this method was successfully applied to high-spin states along several isotopic chains with $I^\pi = 13/2^+, 11/2^-$, and $9/2^+$.

In the present work, we use the self-consistent theory of finite Fermi systems (TFFS) [24] based on the Fayans DF3-a functional [25–27] for calculating μ across long isotopic chains. The basics of our approach can be found in Refs. [10,28,29]. The same framework has also been applied for describing nuclear radii [25] and β decay [30]. Here, this approach has been substantially extended compared to its previous applications. It will be shown that the TFFS can qualitatively reproduce both the general trend, and the pronounced irregularities at $N = 126$ that our experiment revealed in the evolution of the μ values in the thallium chain.

2. Experimental details

Radioactive thallium isotopes were produced in spallation reactions by a 1.4-GeV proton beam (average intensity up to 2 μA) from the CERN proton synchrotron booster bombarding a 50 g/cm^2 UC_x target. The reaction products diffused through the target material, kept at a temperature of $\sim 2000\,^\circ$C, and effused into the hot ion-source cavity as neutral atoms. At the masses of interest ($A = 207-209$), very strong isobaric contamination from surface-ionized francium is present, which prevented extensions of earlier experiments to heavier masses. The yields of francium isotopes at $A = 207-209$ are $> 10^7$ ions/μC [31,32], several orders of magnitude above the production rate of isobaric thallium nuclei (see Sec. 2.1). To overcome this problem, the LIST was used [16–18]. It separates the regions of laser and surface ionization by using a positively charged repeller electrode positioned immediately downstream of the hot cavity at the entrance of the LIST. This suppresses the flow of ions from the cavity, including those of surface-ionized francium. Only neutral atoms may diffuse into the ion guide of the LIST, where laser ionization of thallium isotopes takes place.

Inside the LIST, thallium atoms were resonantly ionized when the laser beams were wavelength-tuned to the two-step thallium ionization scheme:

$$6p^2P_{1/2} \xrightarrow[\text{LiopStar}]{277\,\text{nm}} 6d^2D_{3/2} \xrightarrow[\text{Blaze}]{532\,\text{nm}} \text{continuum}. \quad (1)$$

The excitation of the $6p^2P_{1/2} \rightarrow 6d^2D_{3/2}$ transition was performed by a frequency-doubled tunable dye laser (LIOP-TEC LiopStar) beam at 277 nm with a linewidth of ≈3 GHz. This transition was scanned to map out the hfs spectra. The subsequent ionization step was provided by a frequency doubled Nd:YVO_4 laser (Lumera Blaze).

In our experiment, the francium ions were suppressed by a factor of $\sim 10^4$ (see Fig. 1 in Supplementary Materials). At the same time, the laser-ionized thallium isotopes were suppressed by a factor of ~20, relative to normal RILIS operation without the LIST [17]. These losses are mostly due to the reduced spatial overlap of the thallium atoms and the laser beam inside the LIST cavity. The improved signal-to-background ratio was the key condition which allowed us to perform our measurements.

After ionization, the thallium ions were extracted and accelerated by a 50-kV electrostatic potential, and mass-separated by the ISOLDE general purpose separator (GPS). The ions were then delivered to either a Faraday cup (FC) or the ISOLDE Decay Station (IDS) [33] for ion counting. The ion current of the stable isotopes ^{203,205}Tl from a dedicated

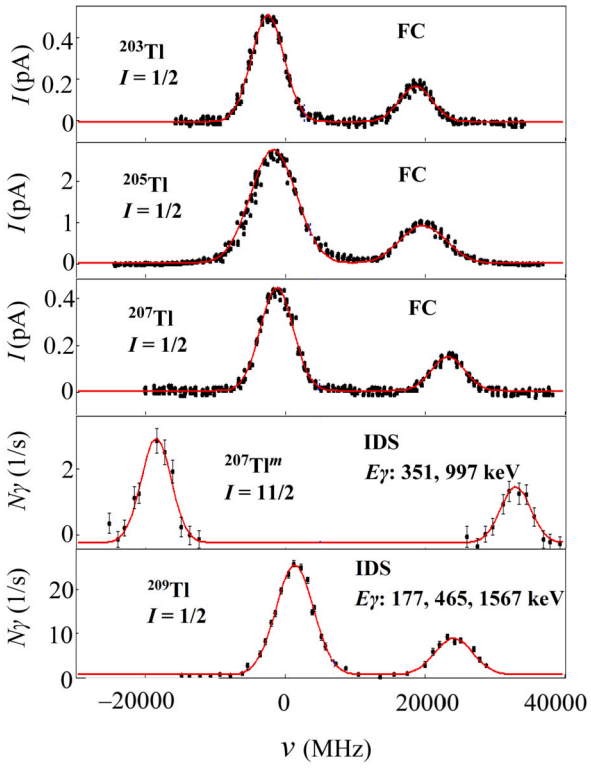

Fig. 1. The hfs of studied thallium isotopes. The solid red lines are Voigt profile fits of the data. The nuclear spin and photoion detection method (FC or IDS), as well as γ-ray energies [34] in the case of decay-based detection at IDS, are displayed for each isotope. The zero point on the frequency scale corresponds to a wavenumber of 36117.92 cm^{-1}. The ion current of the stable isotopes ^{203,205}Tl was produced by the heating of the dedicated oven.

Table 1
Measured yields for thallium isotopes using the LIST. Uncertainties are estimated as 30%.

Nucleus	Ions/μC
^{207}Tl^{g}	5.5×10^{6}
^{207}Tl^{m}	3.4×10^{1}
^{208}Tl	1.5×10^{4}
^{209}Tl	3.2×10^{2}

oven, as well as abundantly produced ^{207}Tl^{g}, were directly measured by the FC as reference scans to validate the stability of the laser. ^{205}Tl was used to regularly check the stability of thallium production and LIST performance.

At the IDS setup, the short-lived isotopes ^{207m,209}Tl were implanted onto a movable aluminized mylar tape which removed longer-lived contamination due to the decay products of the isotopes of interest (for example, $T_{1/2}(^{209}\text{Pb}) = 3.2$ h). The production rate of thallium isotopes was measured via their β-delayed or internal transition (IT) γ rays with six high purity Germanium clover detectors at IDS. Fig. 1 shows examples of the hfs spectra, whereby the count rate in FC or IDS is plotted as a function of the frequency of the scanning laser.

2.1. Production yields for $^{207-209}$Tl

Table 1 summarizes the thallium yields measured in this work. We note that a target unit that had been employed in the previous experimental campaigns was used for the present study. Typically this re-use results in lower production yields than with the new targets.

The sudden drop in yield between ^{208}Tl and ^{209}Tl was due to a difference in indirect, in-target production. A significant amount of ^{208}Tl originated from the α decay of ^{212}Bi ($T_{1/2} \approx 1$ h, $b_\alpha \approx 36\%$), which was produced in the target both directly and via the in-target decay of the abundantly-produced precursors (^{216}At, ^{220}Fr). The analogous $^{213}\text{Bi}\rightarrow^{209}$Tl decay has a branching ratio of only $b_\alpha \approx 2\%$.

Table 2
Magnetic hfs constants for the atomic ground state $6p^2P_{1/2}$ (a_1) and magnetic moments (μ) of thallium isotopes. Where available, literature values are shown in a second line for each isotope.

A	I	a_1(MHz)	$\mu(\mu_N)$
203	1/2	21180(102)	1.622(8)
		21105.4497638(5) [36]	1.616(2) [8]
205	1/2	21302(46)	1.631(4)
		21310.835(5) [37]	1.632(2) [8]
207 g	1/2	24398(44)	1.868(6)
		24690(300) [13]	1.869(5) [8]
207 m	11/2	8391(85)	7.045(84)
209	1/2	22650(330)	1.735(28)

3. Data analysis and results

3.1. Fitting of the hyperfine-structure spectra

The data analysis procedure was the same as in our previous studies of the neutron-deficient thallium isotopes ($A = 179 - 207$) [13,14]. The positions of the hyperfine components in the hfs spectra are determined by the standard relation [13] with five parameters: nuclear spin (I), isotope shift relative to the stable ^{205}Tl ($\delta\nu^{A,205}_{277\,\text{nm}}$), magnetic hfs constants (a_1 and a_2) for the first and the second level of the ionization scheme, and the electric quadrupole hfs constant b_2 for the second level. Note that $b_1 \equiv 0$, since the first level in the ionization scheme has electronic angular momentum $J = 1/2$.

Voigt profiles were fitted to the experimental hfs spectra [13,14], using a fixed $a_2/a_1 = -0.002013(19)$ ratio taken from the value for the stable isotope ^{205}Tl [35], and I values from [34].

For ^{207}Tl^{m} with $I = 11/2$, the possible quadrupole splitting of the upper level $6d^2D_{3/2}$ of the scanned transition should be taken into account. There are no experimental data on the hfs quadrupole constant b_2 for this level in the thallium atom, therefore we made dedicated atomic calculations.

The hyperfine constant b is related to the spectroscopic quadrupole moment Q_s via the equation: $b = eQ_s \times V$, where V is the electric field gradient (EFG) produced by the electrons at the site of the nucleus. The value of the EFG for the $6d^2D_{3/2}$ level, $V = 41.2(23)$ MHz/b, was calculated by employing the relativistic coupled cluster theory and the Dirac-Coulomb Hamiltonian (see details in Supplementary Materials).

^{207}Tl^{m} is a nucleus with a single proton hole in a doubly magic ^{208}Pb. Correspondingly, its quadrupole moment should be less than that of nuclei with the same configuration and moderate deformation (e.g. $I^\pi = 11/2^-$ isomers in ^{197,195,193}Au, all having $|Q_s| < 2$ b, see [38]). Thus, we assume $|Q_s(^{207}\text{Tl}^m)| < 2$ b as an estimate for the calculations.

Using the calculated EFG, one obtains $b(6d^2D_{3/2}; ^{207}\text{Tl}^m) < 83$ MHz. To test the sensitivity to the b_2 value, we fitted the ^{207}Tl^{m} hfs with $b_2 = 0$ and $b_2 = 83$ MHz assumptions. The resulting difference in the a constant is ~ 3 MHz, thus, the influence of the $6d^2D_{3/2}$-state quadrupole splitting on the fitting result is negligible relative to our experimental precision.

In Table 2, the $a(6p^2P_{1/2})$ constant for the studied thallium isotopes are shown, along with values from literature. Our results for ^{203,205,207}Tl^{g} agree with literature data fairly well.

3.2. Magnetic dipole moments

Based on the known values of $\mu_{205} = 1.632(2)\ \mu_N$ [8], $a_{205} = 21310.835(5)$ MHz [37] and $I_{205} = 1/2$ of stable ^{205}Tl, the μ values for thallium isotopes were evaluated using the relation:

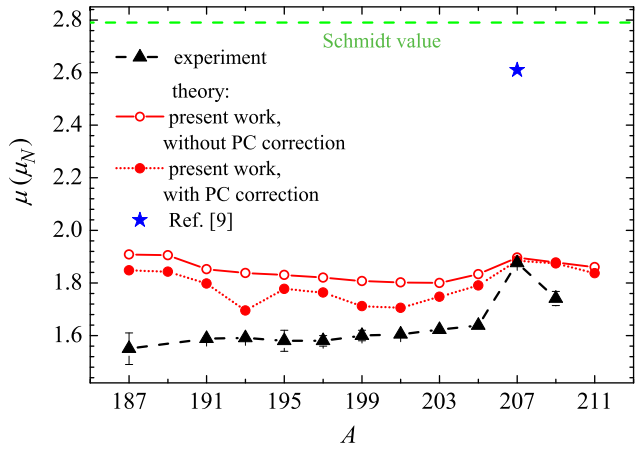

Fig. 2. The μ values for $1/2^+$ ground states in thallium isotopes. The black triangles are experimental data from [41] and the present work (^{209}Tl). The blue star is the theoretical value from [9]. The closed and open circles show our DF3-a+CQRPA calculations results with and without PC correction. The green dashed line marks the Schmidt value for the $\pi s_{1/2}$ state.

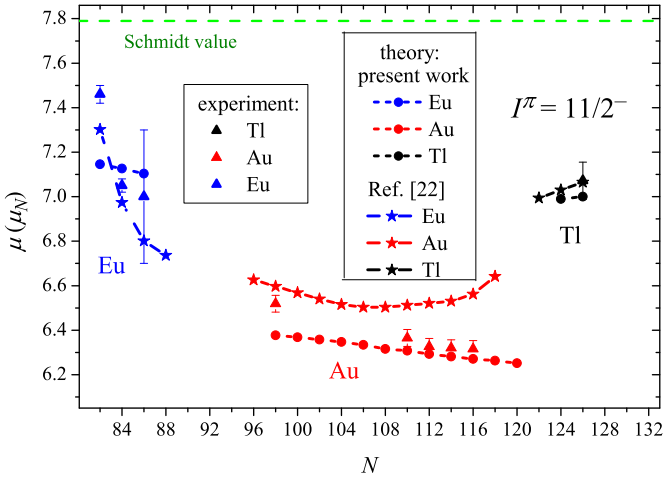

Fig. 3. The μ values for the $11/2^-$ states in europium ($Z = 63$), gold ($Z = 79$), and thallium ($Z = 81$) isotopes. The triangles are experimental data from [39, 41] and the present work (^{207}Tl^m), the stars are theoretical values from [22], and the circles are theoretical values from the present work. The green dashed line marks the Schmidt value for the $\pi h_{11/2}$ state.

$$\mu_A = \mu_{205} \cdot \frac{I_A}{I_{205}} \cdot \frac{a_A(6P_{1/2})}{a_{205}(6P_{1/2})} \cdot [1 + {}^{205}\Delta^A(6P_{1/2})] \tag{2}$$

where $^{205}\Delta^A(6P_{1/2})$ is the relative hyperfine anomaly (RHFA) for the $6p^2P_{1/2}$ atomic state.

The RHFA for ^{207,209}Tl^g were estimated in accordance with the procedure outlined in Ref. [39] taking into account that the hyperfine anomaly reveals itself in the change in the ratio of the magnetic hfs constants for different atomic states (see details in Supplementary Materials): $|^{205}\Delta^{207}(6P_{1/2})| < 1.2 \cdot 10^{-3}$, $|^{205}\Delta^{209}(6P_{1/2})| < 1.2 \cdot 10^{-3}$.

The RHFA for the $\pi h_{11/2}$ state in ^{207}Tl was estimated using the RHFA for the $\pi h_{9/2}$ state in thallium, deduced from experimental data [40], and the single-particle approximation for the ratio of the RHFA values for the $\pi h_{9/2}$ and $\pi h_{11/2}$ shell-model states (see details in Supplementary Materials): $^{205}\Delta^{207m}(6P_{1/2}) = -0.0033(16)$.

The magnetic moments of ^{209}Tl and ^{207}Tl^m were determined for the first time; they are presented in Table 2 and in Figs. 2, 3 along with the previously measured μ values for the thallium ground states (Fig. 2), as well as gold and europium $11/2^-$ isomers (Fig. 3).

The new result for $\mu(^{209}\text{Tl};\ N = 128)$, shows that there is a maximum at $N = 126$, with a less pronounced decrease in μ when going from $N = 126$ to $N = 128$, compared to that when going from $N = 126$ to $N = 124$.

3.2.1. *Renormalization of the proton orbital g factor*

Our new data for ^{207}Tl^m provide further insight into the proton orbital gyromagnetic factor g_ℓ near ^{208}Pb. Earlier studies showed that in order to describe μ values associated with single-particle orbitals near ^{208}Pb, an effective value $g_\ell^{\text{eff}} \sim 1.1$ is needed instead of the free-proton value $g_\ell = 1$ [24,42–44]. The magnetism connected with the orbital motion of nucleons is one of the few nuclear properties at low excitation energy directly connected with mesonic exchange currents (see, for example, Refs. [45–48] and references therein).

Previous estimations of the "experimental" g_ℓ^{eff} factor stemmed from considerations of single-particle high-spin states g factors ($g = \mu/I$), but some were extracted from the measured g factors of two-particles excited states using the additivity relation for magnetic moments ([42–44,49,50] and references therein) rather than from direct measurements. However, the usage of the additivity relation introduces a poorly defined uncertainty. Indeed, there are well-known cases where additivity does not work, see for example, the systematics of g factors for $h^n_{9/2}$ states in the $N = 126$ isotones [51–53], or the strong and so far unexplained violation of additivity in ^{196,198}Au^m, $I^\pi = 12^-$ [54,55]. In contrast to this, our approach with directly measured $\mu(^{207}\text{Tl}^m; \pi h_{11/2})$, is free from this indeterminacy.

We follow the suggestion made in Refs. [49,56], that the measurement of the g factors of the two spin-orbit partners (e.g. $\pi h_{11/2}$ and $\pi h_{9/2}$) in a doubly magic ± 1 particle nuclei gives, with a good approximation, the value of the effective g_ℓ factor:

$$g(j = \ell + 1/2) + g(j = \ell - 1/2) = 2g_\ell^{\text{eff}}. \tag{3}$$

Our measurement of $\mu(^{207}\text{Tl}^m; \pi h_{11/2}) = 7.045(84)\ \mu_N$ [$g(\pi h_{11/2}) = 1.281(15)$] allows us to implement this procedure for the first time, taking into account that $\mu(^{209}\text{Bi}^g; \pi h_{9/2}) = 4.0900(15)\ \mu_N$ [$g(\pi h_{9/2}) = 0.9089(3)$] was measured earlier [57]:

$$g_\ell^{\text{eff}} = [g(\pi h_{11/2}) + g(\pi h_{9/2})]/2 = 1.095(11) \tag{4}$$

Thus, our result supports the previously proposed renormalized value $g_l^{\text{eff}} = 1.115(20)$ [49].

4. Theoretical calculations

The experimental data were compared with theoretical calculations performed within the framework of the self-consistent finite Fermi-system theory [24]. The nuclear ground state is constructed in the spherical EDF approach using the DF3-a functional by Fayans et al. [25–27].

The self-consistent feedback between the core deformation and static polarization induced by unpaired nucleon is given by the TFFS effective field. It is determined from the continuum quasiparticle random-phase-like (CQRPA) equations with the effective NN-interaction taken as the Landau-Migdal spin-dependent interaction augmented with the one-pion and rho-meson exchange modified by the nuclear medium [10]. Solving these equations directly in coordinate space allows one to exactly take into account the single-particle continuum in nuclei with pairing correlations.

In our calculation, the CQRPA part of this framework has been substantially extended compared to its previous application in Refs. [10,28, 29]). A zero-range density-dependent surface pairing is used in diagonal HFB approximation on the extended base including the quasi-discrete states up to $E_{\text{Fermi}} = 37$ MeV.

On the top of CQRPA, the higher-order quasiparticle-phonon coupling (PC) correction was included. Notice, that there are two types of PC corrections: "regular", which is supposed to be included into the

standard TFFS parameters, and "non-regular" (A, Z and state dependent) which should be calculated separately. In order to avoid double counting, regular corrections should be excluded in the PC-contribution calculations. We used a special procedure developed in [29] to account for non-regular PC contributions in the so-called g_L^2 approximation of the perturbation theory (here g_L is the L-phonon creation amplitude, not to be confused with g_ℓ gyromagnetic factor).

To trace the N dependence of the $\mu(11/2^-)$ values in the odd-Z isotopic chains, we also calculated μ for several gold and europium isomers. For the gold isotopic chain where deformation is non-negligible, the standard kinematic factors correction [10] is added within the particle-rotator model [58].

It should be stressed that in the present calculations we did not introduce or redefine any model parameters which were fixed in [10,28].

5. Discussion

In Fig. 2 the results of our DF3-a+CQRPA calculations for the ground state μ values of $^{187-211}$Tl ($I^\pi = 1/2^+$) are compared to experimental data.

The result for ^{209}Tl^g ($N = 128$) proves to be rather unexpected. Namely, it was suggested earlier [11] that in order to explain the jump in magnetic moments of the $1/2^+$ thallium state when going from $N = 124$ to $N = 126$, the particle-vibration coupling (PVC) should be taken into account. The justification of this suggestion is straightforward. Indeed, the energy of the 2_1^+ phonon of the doubly-magic ^{208}Pb core (4.085 MeV) is markedly higher than in lead isotopes with $N < 126$ (0.803 MeV for $N = 124$; 0.899 MeV for $N = 122$ etc.). Keeping in mind that $E(2_1^+, {}^{210}\mathrm{Pb}_{128}) = 0.800$ MeV, i.e. is similar to $E(2_1^+, {}^{206}\mathrm{Pb}_{124})$, one can expect that the PVC effect will be the same for $^{209}\mathrm{Tl}_{128}$ and $^{205}\mathrm{Tl}_{124}$, that is, $\mu(^{209}\mathrm{Tl}^g)$ should be close to $\mu(^{205}\mathrm{Tl}^g)$. However, the decrease of μ when going from $N = 126$ to $N = 124$ (0.24 μ_N) proves to be nearly two times larger than that when going from $N = 126$ to $N = 128$ (0.13 μ_N). This "asymmetry" casts doubt on the completeness of the conventional PVC explanation of the μ irregularity in thallium isotopes near magic $N = 126$.

Our calculations without the PC correction (open circles in Fig. 2) reproduce the general trend with mean deviation of ≈ 0.2 μ_N ($\approx 13\%$). However, in these variant the increase at $N = 126$ practically disappears. Accounting for the PC correction (full circles in Fig. 2) decreases the mean deviation from experiment to ≈ 0.13 μ_N. The reduction of μ either side of the magic number is qualitatively reproduced, although the size of the decrease is still half of the experimental one. The smoother N-dependence of the DF3-a+CQRPA μ values, as well as the better overall agreement with experiment compared to the earlier calculations in Ref. [29] has been achieved due to the inclusion of the quasi-discrete states with $E \lessapprox E_{\mathrm{Fermi}}$ in the pairing calculation.

Importantly, $\mu_{\mathrm{expt}}(^{207}\mathrm{Tl}^g) = 1.869(5)$ μ_N is well described within the DF3-a+CQRPA approach (1.897 μ_N) with a deviation from the experiment of just 0.028(5) μ_N. This agreement can be mainly ascribed to exact accounting for the particle-hole continuum and taking into account the meson exchange current effects in the external field operator, as well as the one-pion exchange in the effective NN-interaction.

Fig. 2 also shows the calculated value of $\mu(^{207}\mathrm{Tl}^g)$ from the recent DEDF study [9]. This value of $\mu(^{207}\mathrm{Tl}^g) = 2.61(2)$ μ_N strongly deviates from the experimental data. This is highlighted in Fig. 2, which demonstrates the departure of this point from the experiment. As indicated in Ref. [9], ^{207}Tl belongs to the group of "outliers" (^{57}Ni, ^{133}Sb, ^{207}Tl, ^{209}Bi) in their calculations, for which the calculated values strongly deviate from experiment (79%, 29%, 39%, 25%, respectively). At the same time, these nuclei do not present any peculiarity for DF3-a+CQRPA calculations and have the "standard" deviation from the experimental data (11%, 12%, 1%, 11%, respectively, see Ref. [10]).

The key point of the DEDF calculations in Ref. [9] is the assumption that the magnetic moments of odd-A nuclei can be analyzed in terms of the self-consistent polarization effects caused by the presence of the unpaired nucleon. In other words, the polarization responsible for the deviation of μ from the Schmidt value is supposed to be exhaustively taken into account already at the deformed mean-field level. The disagreement with experiment for the "outliers" was attributed to the presence of configuration mixing that is not fully taken into account in the mean-field calculations [9]. In contrast with such an approach, in the TFFS calculations the first-order polarization produced by the odd nucleon is described by the CQRPA equations developed on the basis of the spherical self-consisted mean field. The quasiparticle-phonon coupling is responsible for the higher-order polarization effects. From the TFFS point of view the disagreement of the DEDF results with the experiment for the "outliers" could be mostly explained by the underestimation of the polarization in the pure mean-field approach. Indeed, in the earlier version of the TFFS [24] there was nearly the same strong discrepancy between the theoretical and experimental results for ^{207}Tl^g (2.5 μ_N [24], 2.6 μ_N [9] versus the experimental value of 1.869(5) μ_N). However, it was shown that a more accurate solving of the CQRPA equation with exact accounting for the single-particle continuum completely removes this discrepancy ([10]; see also Table 2).

Our DF3-a+CQRPA calculation has shown that the CQRPA polarization is responsible for 66% of the deviation of $\mu(^{207}\mathrm{Tl}^g)$ from the Schmidt value. For comparison, the TFFS calculation performed for Sly4 functional [59] results in a similar value of 61%. Note, that the absolute values of $\mu(^{207}\mathrm{Tl}^g)$ in both calculations are in good agreement with the experiment (DF3-a+CQRPA: 1.897 μ_N; Sly4-TFFS: 1.884 μ_N).

Another substantial mechanism of the μ reduction within the TFFS is connected with the so-called local charges arising due to a nuclear-medium-induced change in the meson exchange currents and the multiparticle many-body diagrams [10,24]. In our DF3-a+CQRPA calculations, this "medium polarization" gives the remaining 34% of the deviation from the Schmidt value (the Sly4-TFFS calculation gives 33%). Both types of polarization seem to be missed in the pure mean-field DEDF approach.

In Fig. 3 the results of our DF3-a+CQRPA calculations for the europium, gold and thallium $11/2^-$ isomers are compared with experimental values. The calculations describe the N dependence of the μ values well, spanning the range of $N = 82 - 126$ with the pronounced maxima at the magic numbers.

In Fig. 3 the results of the DEDF calculations [22] are also shown. The DEDF and TFFS approaches display a comparable accuracy in describing the $11/2^-$ isomers.

Notice, that the relatively small CQRPA-polarization effect is induced by the $M1$-fields in this case. The absolute value of this polarization amounts to only 9% of the difference between the Schmidt value and the experiment for the Sly4-TFFS calculation of ^{207}Tl^m [59]. This is in contrast to the much stronger CQRPA polarizaton for the $1/2^+$ state, which presents a greater challenge for theoretical models, as explained above.

A "self-consistent" polarization correction due to time-odd fields was suggested earlier in [19] within the relativistic covariant density functional theory (CDFT). The contribution of this polarization to μ was calculated as the difference between μ of triaxially deformed CDFT and μ of spherical CDFT. As in the DEDF, it turned to be insufficient to explain the deviation from the Schmidt value. An agreement with the experiment for ^{207}Tl^g, as well as for other doubly magic ± 1 particle nuclei, was achieved only after taking into account the beyond mean-field contributions (meson exchange currents, first- and second-order polarization corrections) [6,19].

6. Conclusion

The μ values for ^{207}Tl^m ($I^\pi = 11/2^-$) and ^{209}Tl^g ($I^\pi = 1/2^+$) have been measured for the first time, using laser resonance-ionization spectroscopy in the LIST device at ISOLDE (CERN).

Self-consistent DF3-a+CQRPA calculations taking into account the meson exchange in the external field operator and effective NN-

interaction, as well as regular effects of $np-nh$ configurations and non-regular PC corrections, have shown an improved description of the μ values in the long isotopic chain of $1/2^+$ ground states in thallium isotopes. The calculations agree fairly well with the general experimental trend, and qualitatively reproduce the "asymmetric" jump at $N=126$ revealed by our measurement of $\mu(^{209}\mathrm{Tl})$.

However, the calculations still underestimate the jump at $N=126$. Note, that "regular" PC corrections were disregarded to avoid double counting, since these corrections are supposed to be included into the standard TFFS parameters. The discarding criteria should be refined in order to check whether the omitted corrections will enable better agreement with experiment.

In this context, the development of the so-called "subtraction method" in Ref. [60] may be effective for ensuring a stable computational scheme for the μ values. Fully consistent systematic calculations of the electromagnetic moments including all corrections beyond the g_L^2 approximation remain to be developed.

The calculations also describe the N dependence of the μ values for the $11/2^-$ isomers fairly well, spanning the range of $N=82-126$. In order to check the predictive power of the theory it would be important to fill the gaps in the $\mu(\pi h_{11/2})$ systematics, namely, to measure magnetic moments for the known long-lived $11/2^-$ states in $^{167-173,193-197}\mathrm{Ir}_{90-96,116-120}$, $^{141}\mathrm{Eu}_{78}$, $^{205}\mathrm{Au}_{126}$.

Declaration of competing interest

The authors declare that they have no known competing financial interests or personal relationships that could have appeared to influence the work reported in this paper.

Data availability

Data will be made available on request.

Acknowledgements

We would like to acknowledge the support of the ISOLDE collaboration and technical teams. The work was supported by the STFC Grants Nos. ST/V001035/1, ST/V001108/1, ST/V001027/1 and ST/P004598/1, by the Romanian Nucleu project No. PN 23 21 01 02 and Institutul de Fizică Atomică (IFA) grant CERN/ISOLDE, by the Research Foundation Flanders (FWO, Belgium), by BOF KU Leuven (C14/22/104), by the Spanish funding agency MICIN/AEI (FEDER, EU) via projects Nos. RTI2018-098868-B-I00 and PID2021-126998OB-I00, by German BMBF under contract 05P21PKCI1 and Verbundprojekt 05P2021, by the Polish Ministry of Education and Science under Contract No. 2021/WK/07, and by the Polish National Science Center under Grant No. 2020/39/B/ST2/02346. M. Au acknowledges funding from the European's Union Horizon 2020 Research and Innovation Program under grant agreement number 861198 project 'LISA' (Laser Ionization and Spectroscopy of Actinides) Marie Skłodowská-Curie Innovative Training Network (ITN). M. Piersa-Siłkowska acknowledges funding from the European Union's Horizon 2020 Research and Innovation Programme under the Marie Skłodowska-Curie grant agreement No. 101032999, "BeLaPEx".

Appendix A. Supplementary material

Supplementary material related to this article can be found online at https://doi.org/10.1016/j.physletb.2024.138452.

References

[1] X. Yang, S. Wang, S. Wilkins, R. Garcia Ruiz, Laser spectroscopy for the study of exotic nuclei, Prog. Part. Nucl. Phys. 129 (2023) 104005, https://doi.org/10.1016/j.ppnp.2022.104005.

[2] A. Barzakh, A.N. Andreyev, C. Raison, J.G. Cubiss, P. Van Duppen, S. Péru, S. Hilaire, S. Goriely, B. Andel, S. Antalic, M. Al Monthery, J.C. Berengut, J. Bieroń, M.L. Bissell, A. Borschevsky, K. Chrysalidis, T.E. Cocolios, T. Day Goodacre, J.-P. Dognon, M. Elantkowska, E. Eliav, G.J. Farooq-Smith, D.V. Fedorov, V.N. Fedosseev, L.P. Gaffney, R.F. Garcia Ruiz, M. Godefroid, C. Granados, R.D. Harding, R. Heinke, M. Huyse, J. Karls, P. Larmonier, J.G. Li, K.M. Lynch, D.E. Maison, B.A. Marsh, P. Molkanov, P. Mosat, A.V. Oleynichenko, V. Panteleev, P. Pyykkö, M.L. Reitsma, K. Rezynkina, R.E. Rossel, S. Rothe, J. Ruczkowski, S. Schiffmann, C. Seiffert, M.D. Seliverstov, S. Sels, L.V. Skripnikov, M. Stryjczyk, D. Studer, M. Verlinde, S. Wilman, A.V. Zaitsevskii, Large shape staggering in neutron-deficient Bi isotopes, Phys. Rev. Lett. 127 (2021) 192501, https://doi.org/10.1103/PhysRevLett.127.192501.

[3] T. Day Goodacre, A.V. Afanasjev, A.E. Barzakh, B.A. Marsh, S. Sels, P. Ring, H. Nakada, A.N. Andreyev, P. Van Duppen, N.A. Althubiti, B. Andel, D. Atanasov, J. Billowes, K. Blaum, T.E. Cocolios, J.G. Cubiss, G.J. Farooq-Smith, D.V. Fedorov, V.N. Fedosseev, K.T. Flanagan, L.P. Gaffney, L. Ghys, M. Huyse, S. Kreim, D. Lunney, K.M. Lynch, V. Manea, Y. Martinez Palenzuela, P.L. Molkanov, M. Rosenbusch, R.E. Rossel, S. Rothe, L. Schweikhard, M.D. Seliverstov, P. Spagnoletti, C. Van Beveren, M. Veinhard, E. Verstraelen, A. Welker, K. Wendt, F. Wienholtz, R.N. Wolf, A. Zadvornaya, K. Zuber, Laser spectroscopy of neutron-rich ^{207,208}Hg isotopes: illuminating the kink and odd-even staggering in charge radii across the $N=126$ shell closure, Phys. Rev. Lett. 126 (2021) 032502, https://doi.org/10.1103/PhysRevLett.126.032502.

[4] G. Neyens, Nuclear magnetic and quadrupole moments for nuclear structure research on exotic nuclei, Rep. Prog. Phys. 66 (4) (2003) 633, https://doi.org/10.1088/0034-4885/66/4/205.

[5] H. Hübel, Kernstrukturaussagen magnetischer momente von hochspinzuständen, Fortschr. Phys. 25 (1977) 327–371, https://doi.org/10.1002/prop.19770250110.

[6] J. Li, J. Meng, Nuclear magnetic moments in covariant density functional theory, Front. Phys. 13 (2018) 132109, https://doi.org/10.1007/s11467-018-0842-7.

[7] R. Neugart, H.H. Stroke, S.A. Ahmad, H.T. Duong, H.L. Ravn, K. Wendt, Nuclear magnetic moment of ^{207}Tl, Phys. Rev. Lett. 55 (1985) 1559–1562, https://doi.org/10.1103/PhysRevLett.55.1559.

[8] N. Stone, Table of recommended nuclear magnetic dipole moments: Part I - Long-lived States, Tech. Rep. INDC(NDS)-0794, International Atomic Energy Agency, 2019, https://www-nds.iaea.org/publications/indc/indc-nds-0794.

[9] P.L. Sassarini, J. Dobaczewski, J. Bonnard, R.F. Garcia Ruiz, Nuclear DFT analysis of electromagnetic moments in odd near doubly magic nuclei, J. Phys. G, Nucl. Part. Phys. 49 (11) (2022) 11LT01, https://doi.org/10.1088/1361-6471/ac900a.

[10] I.N. Borzov, E.E. Saperstein, S.V. Tolokonnikov, Magnetic moments of spherical nuclei: status of the problem and unsolved issues, Phys. At. Nucl. 71 (3) (2008) 469, https://doi.org/10.1134/S1063778808030095.

[11] A. Arima, H. Sagawa, The effect of particle-vibration coupling due to the collective 2^+ state on the magnetic moments of Tl isotopes, Phys. Lett. B 173 (4) (1986) 351–354, https://doi.org/10.1016/0370-2693(86)90392-8.

[12] J.A. Bounds, C.R. Bingham, H.K. Carter, G.A. Leander, R.L. Mlekodaj, E.H. Spejewski, W.M. Fairbank, Nuclear structure of light thallium isotopes as deduced from laser spectroscopy on a fast atom beam, Phys. Rev. C 36 (1987) 2560–2568, https://doi.org/10.1103/PhysRevC.36.2560.

[13] A.E. Barzakh, L.K. Batist, D.V. Fedorov, V.S. Ivanov, K.A. Mezilev, P.L. Molkanov, F.V. Moroz, S.Y. Orlov, V.N. Panteleev, Y.M. Volkov, Changes in the mean-square charge radii and magnetic moments of neutron-deficient Tl isotopes, Phys. Rev. C 88 (2013) 024315, https://doi.org/10.1103/PhysRevC.88.024315.

[14] A.E. Barzakh, A.N. Andreyev, T.E. Cocolios, R.P. de Groote, D.V. Fedorov, V.N. Fedosseev, R. Ferrer, D.A. Fink, L. Ghys, M. Huyse, U. Köster, J. Lane, V. Liberati, K.M. Lynch, B.A. Marsh, P.L. Molkanov, T.J. Procter, E. Rapisarda, S. Rothe, K. Sandhu, M.D. Seliverstov, A.M. Sjödin, C. Van Beveren, P. Van Duppen, M. Venhart, M. Veselský, Changes in mean-squared charge radii and magnetic moments of $^{179-184}$Tl measured by in-source laser spectroscopy, Phys. Rev. C 95 (2017) 014324, https://doi.org/10.1103/PhysRevC.95.014324.

[15] R. Catherall, W. Andreazza, M. Breitenfeldt, A. Dorsival, G.J. Focker, T.P. Gharsa, T.J. Giles, J.L. Grenard, F. Locci, P. Martins, S. Marzari, J. Schipper, A. Shornikov, T. Stora, The ISOLDE facility, J. Phys. G, Nucl. Part. Phys. 44 (9) (2017) 1, https://doi.org/10.1088/1361-6471/aa7eba.

[16] D. Fink, S. Richter, B. Bastin, K. Blaum, R. Catherall, T. Cocolios, D. Fedorov, V. Fedosseev, K. Flanagan, L. Ghys, A. Gottberg, N. Imai, T. Kron, N. Lecesne, K. Lynch, B. Marsh, T. Mendonca, D. Pauwels, E. Rapisarda, J. Ramos, R. Rossel, S. Rothe, M. Seliverstov, M. Sjödin, T. Stora, C. Van Beveren, K. Wendt, First application of the Laser Ion Source and Trap (LIST) for on-line experiments at ISOLDE, Nucl. Instrum. Methods Phys. Res., Sect. B 317 (2013) 417–421, https://doi.org/10.1016/j.nimb.2013.06.039.

[17] D.A. Fink, T.E. Cocolios, A.N. Andreyev, S. Antalic, A.E. Barzakh, B. Bastin, D.V. Fedorov, V.N. Fedosseev, K.T. Flanagan, L. Ghys, A. Gottberg, M. Huyse, N. Imai, T. Kron, N. Lecesne, K.M. Lynch, B.A. Marsh, D. Pauwels, E. Rapisarda, S.D. Richter, R.E. Rossel, S. Rothe, M.D. Seliverstov, A.M. Sjödin, C. Van Beveren, P. Van Duppen, K.D.A. Wendt, In-source laser spectroscopy with the laser ion source and trap: first direct study of the ground-state properties of ^{217,219}Po, Phys. Rev. X 5 (2015) 011018, https://doi.org/10.1103/PhysRevX.5.011018.

[18] R. Heinke, M. Au, C. Bernerd, K. Chrysalidis, T.E. Cocolios, V.N. Fedosseev, I. Hendriks, A.A. Jaradat, M. Kaja, T. Kieck, T. Kron, R. Mancheva, B.A. Marsh, S. Marzari, S. Raeder, S. Rothe, D. Studer, F. Weber, K. Wendt, First on-line application of

the high-resolution spectroscopy laser ion source PI-LIST at ISOLDE, Nucl. Instrum. Methods Phys. Res., Sect. B 541 (2023) 8–12, https://doi.org/10.1016/j.nimb.2023.04.057.

[19] J. Li, J.X. Wei, J.N. Hu, P. Ring, J. Meng, Relativistic description of magnetic moments in nuclei with doubly closed shells plus or minus one nucleon, Phys. Rev. C 88 (2013) 064307, https://doi.org/10.1103/PhysRevC.88.064307.

[20] V. Tselyaev, N. Lyutorovich, J. Speth, G. Martinez-Pinedo, K. Langanke, P.G. Reinhard, Electric and magnetic moments and transition probabilities in ^{208}Pb ± 1 nuclei, arXiv:2201.08838, 2022.

[21] A.R. Vernon, R.F. Garcia Ruiz, T. Miyagi, C.L. Binnersley, J. Billowes, M.L. Bissell, J. Bonnard, T.E. Cocolios, J. Dobaczewski, G.J. Farooq-Smith, K.T. Flanagan, G. Georgiev, W. Gins, R.P. de Groote, R. Heinke, J.D. Holt, J. Hustings, Á. Koszorús, D. Leimbach, K.M. Lynch, G. Neyens, S.R. Stroberg, S.G. Wilkins, X.F. Yang, D.T. Yordanov, Nuclear moments of indium isotopes reveal abrupt change at magic number 82, Nature 607 (2022) 260, https://doi.org/10.1038/s41586-022-04818-7.

[22] J. Bonnard, J. Dobaczewski, G. Danneaux, M. Kortelainen, Nuclear DFT electromagnetic moments in heavy deformed open-shell odd nuclei, Phys. Lett. B 843 (2023) 138014, https://doi.org/10.1016/j.physletb.2023.138014.

[23] T. Gray, A. Stuchbery, J. Dobaczewski, A. Blazhev, H. Alshammari, L. Bignell, J. Bonnard, B. Coombes, J. Dowie, M. Gerathy, T. Kibédi, G. Lane, B. McCormick, A. Mitchell, C. Nicholls, J. Pope, P.-G. Reinhard, N. Spinks, Y. Zhong, Shape polarization in the tin isotopes near $N = 60$ from precision g-factor measurements on short-lived $11/2^-$ isomers, Phys. Lett. B 847 (2023) 138268, https://doi.org/10.1016/j.physletb.2023.138268.

[24] A. Migdal, Theory of Finite Fermi Systems and Applications to Atomic Nuclei, Wiley, New York, 1967.

[25] E.E. Saperstein, S.V. Tolokonnikov, Self-consistent theory of finite Fermi systems and radii of nuclei, Phys. At. Nucl. 74 (2011) 1277, https://doi.org/10.1134/S1063778811090109.

[26] S. Fayans, S. Tolokonnikov, E. Trykov, D. Zawischa, Nuclear isotope shifts within the local energy-density functional approach, Nucl. Phys. A 676 (1) (2000) 49–119, https://doi.org/10.1016/S0375-9474(00)00192-5.

[27] I.N. Borzov, S.A. Fayans, E. Krömer, D. Zawischa, Ground state properties and β-decay half-lives near ^{132}Sn in a self-consistent theory, Z. Phys. A, Hadrons Nucl. 355 (1) (1996) 117–127, https://doi.org/10.1007/BF02769674.

[28] I.N. Borzov, E.E. Saperstein, S.V. Tolokonnikov, G. Neyens, N. Severijns, Description of magnetic moments of long isotopic chains within the FFS theory, Eur. Phys. J. A 45 (2010) 159, https://doi.org/10.1140/epja/i2010-10985-y.

[29] E.E. Saperstein, O.I. Achakovskiy, S.P. Kamerdzhiev, S. Krewald, J. Speth, S.V. Tolokonnikov, Phonon coupling effects in magnetic moments of magic and semimagic nuclei, Phys. At. Nucl. 77 (2014) 1033, https://doi.org/10.1134/S1063778814080122.

[30] I.N. Borzov, Gamow-Teller and first-forbidden decays near the r-process paths at $N = 50, 82$, and 126, Phys. Rev. C 67 (2003) 025802, https://doi.org/10.1103/PhysRevC.67.025802.

[31] The ISOLDE yield database, version 0.2.1.0 [Online]. https://isoyields2.web.cern.ch/. (Accessed 4 April 2023), 2020.

[32] J. Ballof, J. Ramos, A. Molander, K. Johnston, S. Rothe, T. Stora, C. Düllman, The upgraded ISOLDE yield database - a new tool to predict beam intensities, Nucl. Instrum. Methods Phys. Res., Sect. B 463 (2019) 211, https://doi.org/10.1016/j.nimb.2019.05.044.

[33] ISOLDE decay station [Online]. https://isolde-ids.web.cern.ch/. (Accessed 6 April 2023).

[34] National nuclear data center [Online]. https://www.nndc.bnl.gov/ensdf/. (Accessed 6 April 2023).

[35] G. Hermann, G. Lasnitschka, D. Spengler, Hyperfine structures and level isotope shifts of the $n^2S_{1/2}(n = 7 - 12)$ and $n^2D_{3/2,5/2}(n = 6 - 10)$ levels of ^{203,205}Tl measured by atomic beam spectroscopy, Z. Phys., D At. Mol. Clust. 28 (2) (1993) 127–134, https://doi.org/10.1007/BF01436979.

[36] C. Ekström, G. Wannberg, Y.S. Shishodia, Hyperfine structure and nuclear magnetic moments of some neutron-deficient thallium isotopes, Hyperfine Interact. 1 (1) (1975) 437–458, https://doi.org/10.1007/BF01022475.

[37] A. Lurio, A.G. Prodell, Hfs separations and hfs anomalies in the $^2P_{1/2}$ state of Ga^{69}, Ga^{71}, Tl^{203}, and Tl^{205}, Phys. Rev. 101 (1956) 79–83, https://doi.org/10.1103/PhysRev.101.79.

[38] G. Seewald, E. Hagn, E. Zech, D. Forkel-Wirth, Measurements of the spectroscopic quadrupole moments of the $11/2^-$ isomers ^{193m}Au, ^{195m}Au and ^{197m}Au with MAPON, Nucl. Phys. A 602 (1) (1996) 41–59, https://doi.org/10.1016/0375-9474(96)00090-5.

[39] A.E. Barzakh, D. Atanasov, A.N. Andreyev, M. Al Monthery, N.A. Althubiti, B. Andel, S. Antalic, K. Blaum, T.E. Cocolios, J.G. Cubiss, P. Van Duppen, T.D. Goodacre, A. de Roubin, Y.A. Demidov, G.J. Farooq-Smith, D.V. Fedorov, V.N. Fedosseev, D.A. Fink, L.P. Gaffney, L. Ghys, R.D. Harding, D.T. Joss, F. Herfurth, M. Huyse, N. Imai, M.G. Kozlov, S. Kreim, D. Lunney, K.M. Lynch, V. Manea, B.A. Marsh, Y. Martinez Palenzuela, P.L. Molkanov, D. Neidherr, R.D. Page, M. Rosenbusch, R.E. Rossel, S. Rothe, L. Schweikhard, M.D. Seliverstov, S. Sels, C. Van Beveren, E. Verstraelen, A. Welker, F. Wienholtz, R.N. Wolf, K. Zuber, Hyperfine anomaly in gold and magnetic moments of $I^\pi = 11/2^-$ gold isomers, Phys. Rev. C 101 (2020) 034308, https://doi.org/10.1103/PhysRevC.101.034308.

[40] A.E. Barzakh, L.K. Batist, D.V. Fedorov, V.S. Ivanov, K.A. Mezilev, P.L. Molkanov, F.V. Moroz, S.Y. Orlov, V.N. Panteleev, Y.M. Volkov, Hyperfine structure anomaly and magnetic moments of neutron deficient Tl isomers with $I = 9/2$, Phys. Rev. C 86 (2012) 014311, https://doi.org/10.1103/PhysRevC.86.014311.

[41] N. Stone, Table of nuclear magnetic dipole and electric quadrupole moments, At. Data Nucl. Data Tables 90 (1) (2005) 75–176, https://doi.org/10.1016/j.adt.2005.04.001.

[42] T. Yamazaki, T. Nomura, S. Nagamiya, T. Katou, Anomalous orbital magnetism of proton deduced from the magnetic moment of the 11^- state of ^{210}Po, Phys. Rev. Lett. 25 (1970) 547–550, https://doi.org/10.1103/PhysRevLett.25.547.

[43] T. Yamazaki, Mesonic exchange effect on nuclear magnetic moments and related problems - experimental, in: M. Rho, D.H. Wilkinson (Eds.), Mesons in Nuclei, vol. II, North-Holland, Amsterdam, 1979, p. 652.

[44] A.E. Stuchbery, Gyromagnetic ratios of excited states and nuclear structure near ^{132}Sn, AIP Conf. Proc. 1625 (1) (2014) 52–58, https://doi.org/10.1063/1.4901764.

[45] M. Chemtob, Two-body interaction currents and nuclear magnetic moments, Nucl. Phys. A 123 (2) (1969) 449–470, https://doi.org/10.1016/0375-9474(69)90513-2.

[46] A. Arima, H. Hyuga, Roles of configuration mixing and exchange currents in nuclear magnetic moments and beta decays, in: M. Rho, D.H. Wilkinson (Eds.), Mesons in Nuclei, vol. II, North-Holland, Amsterdam, 1979, p. 684.

[47] M. Rho, Quarks and mesons in nuclei, Nucl. Phys. A 354 (1) (1981) 3–18, https://doi.org/10.1016/0375-9474(81)90590-X.

[48] G. Brown, M. Rho, Velocity dependence of the nucleon-nucleon interaction, exchange currents and enhancement of the dipole sum rule in nuclei, Nucl. Phys. A 338 (2) (1980) 269–280, https://doi.org/10.1016/0375-9474(80)90033-0.

[49] K.H. Maier, J.A. Becker, J.B. Carlson, R.G. Lanier, L.G. Mann, G.L. Struble, T. Nail, R.K. Sheline, W. Stöffl, L. Ussery, g factor of the $J^\pi = 25/2^+$ isomer in ^{205}Tl and the anomalous orbital magnetism of the proton, Phys. Rev. Lett. 48 (1982) 466–469, https://doi.org/10.1103/PhysRevLett.48.466.

[50] J.A. Becker, J.B. Carlson, R.G.I. anier, L.G. Mann, G.L. Struble, K.H. Maier, L. Ussery, W. Stöffl, T. Nail, R.K. Sheline, J.A. Cizewski, 2.102-MeV level in ^{206}Hg and the spin gyromagnetic ratio of the $3s$ proton, Phys. Rev. C 26 (1982) 914–919, https://doi.org/10.1103/PhysRevC.26.914.

[51] I. Towner, F. Khanna, O. Häusser, Magnetic moments in $N = 126$ isotones and core polarisation blocking, Nucl. Phys. A 277 (2) (1977) 285–300, https://doi.org/10.1016/0375-9474(77)90314-1.

[52] O. Häusser, J.R. Beene, T. Faestermann, T.K. Alexander, D. Horn, A.B. McDonald, A.J. Ferguson, Knight shifts and absolute magnetic moments in trans-bismuth nuclei, Hyperfine Interact. 4 (1978) 219, https://doi.org/10.1007/BF01021829.

[53] A. Stuchbery, A. Byrne, G. Dracoulis, B. Fabricius, T. Kibédi, Multiparticle-octupole coupling and magnetic moments of $h^n_{9/2}$ isomers in N = 126 isotones, Nucl. Phys. A 555 (2) (1993) 355–368, https://doi.org/10.1016/0375-9474(93)90291-5.

[54] E. Hagn, E. Zech, Nuclear magnetic moment of the 9.7 h 12^- isomer ^{196m}Au, Nucl. Phys. A 373 (2) (1982) 256–266, https://doi.org/10.1016/0375-9474(82)90150-6.

[55] E. Hagn, E. Zech, Nuclear magnetic moment of 7.8 s $11/2^-$ ^{197m}Au and 2.3 d 12^- ^{198m}Au, Nucl. Phys. A 417 (1) (1984) 88–108, https://doi.org/10.1016/0375-9474(84)90325-7.

[56] F. Petrovich, Effective moment operator for magnetic moments and M1 transitions in the Pb region, Nucl. Phys. A 203 (1) (1973) 65–77, https://doi.org/10.1016/0375-9474(73)90423-5.

[57] S. Schmidt, J. Billowes, M. Bissell, K. Blaum, R. Garcia Ruiz, H. Heylen, S. Malbrunot-Ettenauer, G. Neyens, W. Nörtershäuser, G. Plunien, S. Sailer, V. Shabaev, L. Skripnikov, I. Tupitsyn, A. Volotka, X. Yang, The nuclear magnetic moment of ^{208}Bi and its relevance for a test of bound-state strong-field QED, Phys. Lett. B 779 (2018) 324–330, https://doi.org/10.1016/j.physletb.2018.02.024.

[58] A. Bohr, B. Mottelson, Nuclear Structure, v.II, W.A. Benjamin, Inc., New York, Amsterdam, 1969.

[59] V. Tselyaev, private communication.

[60] V.I. Tselyaev, Subtraction method and stability condition in extended random-phase approximation theories, Phys. Rev. C 88 (2013) 054301, https://doi.org/10.1103/PhysRevC.88.054301.